

Engineering near-surface electron states in three-dimensional topological insulators

V. N. Men'shov^{+*1)}, V. V. Tugushev^{+**×}, E. V. Chulkov^{*°}

⁺National Research Centre "Kurchatov Institute", 123182 Moscow, Russia

^{*}Tomsk State University, 634050 Tomsk, Russia

[×]Prokhorov General Physics Institute of the RAS, 119991 Moscow, Russia

[°]Departamento de Fisica de Materiales, Facultad de Ciencias Quimicas, UPV/EHU and Centro de Fisica de Materiales CFM-MPC, Centro Mixto CSIC-UPV/EHU, 20080 San Sebastian, Basque Country, Spain

Submitted 5 August 2013

Resubmitted 3 October 2013

Using the continual model of a semi-infinite three dimensional (3D) topological insulator (TI) we study the effect of the surface potential (SP) on the formation of helical topological states near the surface. The results reveal that spatial profile and spectrum of these states strongly depend on the SP type and strength. We pay special attention to the 3D TI substrate/non-magnetic insulating overlayer system to illustrate the principles of the topological near-surface states engineering.

DOI: 10.7868/S0370274X13220050

Introduction. The hallmark of three dimensional (3D) topological insulators (TIs) is an existence of unusual so-called topological bound states on the boundary of a TI material with vacuum or at the interface between topologically nontrivial and trivial constituents in a hybrid structure [1, 2]. These states, also known as the Dirac helical states, have many exciting physical properties supported by time-reversal symmetry, such as linear gapless dispersion and spin-moment locking [1–3]. For example, the transport and magneto-transport features of the helical quasiparticles provide original opportunities for different spintronic device applications [4–6]. However, to fully realize these opportunities 3D TIs have to be brought into the contact with the topologically trivial magnetic and non-magnetic insulators or semiconductors. While a rapid progress has been made in investigation of the vacuum-terminated TI surfaces [1–3], it is still challenging to control the properties of topological states under the surface modification in the more complex structures. Recent experiments on 3D TIs have demonstrated that these states are notably sensitive to external influences, such as chemical doping of the surface via deposition of both magnetic and non-magnetic elements [7–9], oxidization of air-exposed samples [10], change of the surface termination [11, 12], capping layers and interfaces with other materials [13, 14], applying an external gate voltage [15, 16], etc.

It is evident that perturbation of a bulk crystal potential near the surface, i.e. the surface potential (SP), exists in the all types of 3D TIs and directly affects the properties of the Dirac states. Even in the absence of an external influence upon the surface, SP can be caused by various factors inherent in the material. For example, the works [17, 18] predict that a real bulk-truncated surface of bismuth-chalcogenides could develop very complex electronic structure in which the topological states coexist with the conventional states of the two-dimensional electron gas (2DEG) in the quantum well appearing near the TI surface due to the band-bending effect. In Ref. [19], the Rashba spin-split surface state with a topological character has been observed, which coexists with a surface Dirac cone in the fundamental bulk gap of Sb_2Te_3 ; the authors associated this finding with a strong internal electric field existing between the utmost surface Te-layer and the subsurface Sb-layer. The *ab initio* calculations [20] have shown that an expansion of the van-der-Waals (vdW) spacing in layered TIs caused by intercalation of deposited atoms leads to a simultaneous emergence of 2DEG bands localized in the subsurface region. Moreover, the expansion of vdW spacing leads also to a relocation of the topological states to the lower quintuple layers [20]. The short-range chemical forces related to dangling-bonds on the surface of a thallium-based ternary chalcogenides (TlBiTe_2 , TlBiSe_2) lead surely to surface modification [21]. The authors of Ref. [22] have

¹⁾e-mail: vnmenshov@mail.ru

studied by first-principle simulation the $\text{Sb}_2\text{Se}_3/\text{Bi}_2\text{Se}_3$ heterostructures, the constituents of which possess the Bloch functions of the same symmetry. They found that the topological state largely moves from the nontrivial Bi_2Se_3 into the region of the trivial Sb_2Se_3 . In Ref. [23] it was established that, depositing a conventional insulator overlayer (ZnM , $M = \text{S}$, Se , and Te) onto the TI substrate (Bi_2Se_3 or Bi_2Te_3), topological states can float to the top of the conventional insulator film, or stay put at the conventional insulator/TI interface, or are pushed down deeper into the otherwise structurally homogeneous TI. In Ref. [24] it was suggested that the Dirac point of helical surface states can be significantly shifted by applying uniaxial strain.

It should be stressed that both experimental and theoretical results show that while the non-topological (conventional) surface states can be created or altered when TI is exposed to ambient conditions or put into the contact with other materials, the topological order itself is robust to these changes and the topological states are not destroyed under the non-drastic external perturbations [25, 26]. However, the characteristics of the topological states can undergo serious changes. For example, the adsorbate-induced bending of the conduction and valence bands near the narrow-gap semiconductor surface is a well-known phenomenon, which has also been observed for some TI surfaces such as $\text{Bi}_2\text{Se}_3(111)$. The studies [7–9] showed that adsorbed metal atoms shift the topological states at this surface to higher binding energies by several hundred meV (possibly due to the band bending effect). Furthermore, the presence of metal adatoms was found to strongly affect the dispersion of the topological states close to the Dirac point, giving rise to its significant deviation from the linearly dispersive behavior [7, 9]. The expansion of the vdW spacings and the detachment of the topmost quintuple layers from the bulk crystal lead to a relocation of topological state beneath the detached quintuple layers [20].

Apart from the aforementioned simulations of the surface properties of 3D TIs based on the first principle approach, various continual models based on the well-known $\mathbf{k} \cdot \mathbf{p}$ method [27] have been discussed to describe relativistic fermions at the TI boundary [28–30]. To approximately characterize the band electron states of a bulk semiconductor, $|n\mathbf{k}\rangle$ (\mathbf{k} is a wave vector, n is a band index), in the region of the Brillouin zone around the point of band extrema \mathbf{k}_0 , the $\mathbf{k} \cdot \mathbf{p}$ method is reputed to be adequate enough. Under a perturbation smooth on the atomic scale, this method makes it possible to qualitatively predict evolution of the electron state wave function $\Psi_n(\mathbf{r})$ in terms of a product of a slowly varying envelope function (EF) $\theta_n(\mathbf{r})$ and the Bloch function

$|n\mathbf{k}_0\rangle = \exp(i\mathbf{k}_0\mathbf{r})u_{n\mathbf{k}_0}(\mathbf{r})$ of the unperturbed crystal at the point \mathbf{k}_0 : $\Psi_n(\mathbf{r}) = \theta_n(\mathbf{r})|n\mathbf{k}_0\rangle$, $u_{n\mathbf{k}_0}(\mathbf{r})$ is the lattice periodic function. The EF concept may also be applied to the description of localized and resonant interface states in the semiconductor junctions of different types. However, a relevant choice of the boundary conditions for the function $\theta_n(\mathbf{r})$ remains an unsettled question in this concept, in particular for the TI based structures. The works [28, 30] impose the so-called “open” boundary conditions fixing all EF components to zero at the crystal surface. This restriction formally simulates the effect of vanishing of the quasiparticle wave function on the infinitely high SP barrier. Nevertheless, it should be pointed out that the zero constraint is not unique, and other options for boundary conditions have been advocated in the literature. For instance, in Ref. [31] the problem is formulated in terms of an energy functional whose minimization yields the so-called “natural” boundary conditions, intermixing the magnitudes and derivatives of different EF components. Both mentioned types of the EF boundary conditions are extremely idealized and cannot adequately take into consideration a sensitivity of the 3D TI electron states to the surface modifications.

In this work we propose a formalism to directly incorporate the surface perturbation effect into the 3D TI Hamiltonian. We derive the appropriate EF boundary conditions through the construction of the effective semi-phenomenological SP localized at the 3D TI surface. The orbital and spin structure of the SP mimics induced fields arising on the surface due to perturbations. As it will be shown below, the structure and strength of the SP determine both the spatial and spectral features of the topological states.

Model Hamiltonian and effective energy functional. Let us discuss the model of a truncated 3D TI covered by an atomically thin non-magnetic insulating overlayer. The low-energy and long-wavelength bulk electronic states of the prototypical 3D TI material Bi_2Se_3 are described in our model by the four band $\mathbf{k} \cdot \mathbf{p}$ Hamiltonian with strong spin orbit coupling (SOC) [28, 29]:

$$H_T(\mathbf{k}) = \Xi(\mathbf{k})\tau_z \otimes \sigma_0 + A\tau_x \otimes (\boldsymbol{\sigma} \cdot \mathbf{k}), \quad (1)$$

where $\Xi(\mathbf{k}) = \Xi - Bk^2$, $\mathbf{k} = (k_x, k_y, k_z)$, $\sigma_{0,x,y,z}$ and $\tau_{0,x,y,z}$ denote the Pauli matrices in the spin and orbital space, respectively; Ξ , B , and A are the model parameters. The Hamiltonian (1) is written in the basis $u = \{|+\uparrow\rangle, |-\uparrow\rangle, |+\downarrow\rangle, |-\downarrow\rangle\}$ of the four states at the Γ point with $\mathbf{k}_0 = 0$. The superscripts \pm denote the even and odd parity states and the arrows $\downarrow\uparrow$ indicate the spin projections onto the z quantization axis. The

model (1) captures the remarkable attribute of the band structure: under the condition Ξ , $B > 0$, the inverted order of the energy terms $|\uparrow(\downarrow)\rangle$ and $|\downarrow(\uparrow)\rangle$ around $\mathbf{k}_0 = 0$, which correctly characterizes the topological nature of the system due to strong SOC. The Hamiltonian (1) is particle-hole symmetric and isotropic, which helps us to simplify calculations.

We consider the system as a semi-infinite slab of the 3D TI material, such as Bi_2Se_3 , occupying the region $z > 0$. The slab boundary located at $z = 0$ is perfectly flat and displays translational symmetry in the (x, y) plane. The potential at the surface of a real 3D TI material is different from the bulk crystal potential, irrespective of whether the surface is kept in ultra-high vacuum or, for example, coated with an overlayer or interfaced with another material. To demonstrate the effect of the surface modification on the topological states within a conceptually simple scheme, we introduce the interaction of electrons with an external perturbation confined at the surface, implementing the effective SP $U(\mathbf{r})$ into the EF calculation. Thus we write the full electron energy of the truncated 3D TI in the following form:

$$\Omega - \int_{z>0} d\mathbf{r} \Theta^+(\mathbf{r}) [H_T(-i\nabla) + U(\mathbf{r})] \Theta(\mathbf{r}). \quad (2)$$

Here, the operator $H_T(-i\nabla)$ determined in Eq. (1) acts in the space of the spinor function $\Theta(\mathbf{r}) = (\theta_1(\mathbf{r}), \theta_2(\mathbf{r}), \theta_3(\mathbf{r}), \theta_4(\mathbf{r}))^{\text{tr}}$ that are represented in the basis u , the superscript tr denotes the transpose operation. The EF components $\theta_j(\mathbf{r})$ (the subscript j numbers the spinor components) are presumed to be smooth and continuous functions in the half-space $z > 0$, while the spatial symmetry and periodicity of the system are broken due to existence of the TI surface. It is evident that the $\mathbf{k} \cdot \mathbf{p}$ approach cannot provide a correct description of the wave-function behavior near the surface, where large momenta are highly important. To overcome this drawback we introduce the effective SP $U(\mathbf{r})$, which affects the electron states of TI at the surface. The potential $U(\mathbf{r})$ is nonzero in a small region d (of the order of a lattice parameter) around the geometrical boundary $z = 0$, where the validity of the $\mathbf{k} \cdot \mathbf{p}$ scheme is questionable. An introduction of the phenomenological SP in Eq. (2) enables us to correctly match the low-energy and long-range electronic states inside the truncated TI with evanescent vacuum states through the boundary conditions for EF $\Theta(\mathbf{r})$. As long as the EF spatial variation of the sought state, $\Theta(\mathbf{r}) = \sum_{\boldsymbol{\kappa}} \Theta(\boldsymbol{\kappa}, z) \exp(i\boldsymbol{\kappa}\boldsymbol{\rho})$ ($\boldsymbol{\kappa} = (k_x, k_y)$, $\boldsymbol{\rho} = (x, y)$), is sufficiently slow in the direction normal to the surface,

one can adopt a local approximation for the SP. Namely one writes $U(\mathbf{r}) = dU(\boldsymbol{\rho})\delta(z + 0)$, where the symbol $+0$ at the argument of the delta-function signifies that the sheet-like SP is placed inside the TI half-space but at infinitesimally small distance from the boundary $z = 0$.

As a matter of course, the “true” wave function has to be continuous at the crystal boundary. Nevertheless, in the system under consideration, since the Bloch factors of the wave function inside and outside TI do not coincide (in particular, they have different space group symmetries), the long-range envelope function $\Theta(\boldsymbol{\kappa}, z)$ can formally undergo a finite discontinuity (jump) across the boundary from $z = 0+$ to $z = 0-$ within the utilized $\mathbf{k} \cdot \mathbf{p}$ method (see Ref. [31]). In the current work, we do not care how the wave function behaves in the half-space $z < 0$ but next make use a variational treatment for the energy functional

$$F\{\Theta^+, \Theta\} = \int_0^\infty dz \Theta^+(\boldsymbol{\kappa}, z) [H_T(\boldsymbol{\kappa}, -i\partial) + dU(\boldsymbol{\kappa})\delta(z + 0) - E] \Theta(\boldsymbol{\kappa}, z), \quad (3)$$

where the energy E plays a role of the Lagrange multiplier. The functional (3) is determined in the class of the smooth and continuous EFs in the TI half-space $z > 0$ and includes the effective surface potential $dU(\boldsymbol{\kappa})\delta(z + 0)$. Since, in a plane geometry, the wave-vector $\boldsymbol{\kappa}$ is a good quantum number, we determine the functional for each EF $\boldsymbol{\kappa}$ -mode, $\Theta(\boldsymbol{\kappa}, z)$, and $\partial = \partial/\partial z$. Varying functional $F\{\Theta^+, \Theta\}$ with respect to the function Θ^+ yields the Euler equations for the half-space $z > 0$ and the boundary conditions at the surface at $z = 0+$. The corresponding equations in the compact form are:

$$[H_T(\boldsymbol{\kappa}, -i\partial) - E] \Theta(\boldsymbol{\kappa}, z) = 0, \quad (4)$$

$$\Pi(\boldsymbol{\kappa}, -i\partial) \Theta(\boldsymbol{\kappa}, 0+) = 2dU(\boldsymbol{\kappa}) \Theta(\boldsymbol{\kappa}, 0+). \quad (5)$$

Here we have introduced the “current” density operator $\Pi(\boldsymbol{\kappa}, k_z) = i\partial H_T(\mathbf{k})/\partial k_z$, which acts on the spinor $\Theta(\boldsymbol{\kappa}, z)$. Thus the right side in Eq. (5) associated with the surface perturbation plays a role of the external (with regard to the TI bulk) “current” source (sink). Equation (5) involves the surface potential parameters, in this sense our approach has something in common with the one used in the study of the surface states of a crystal with the relativistic band structure in Ref. [32]. The solution of the boundary task, Eqs. (4)–(5), answers the principal physical question how the perturbation located just at the TI boundary affects the near-surface topological states.

In the half-space $z > 0$, the general solution of Eq. (4) for each EF spinor component obeying the condition $\theta_j(\boldsymbol{\kappa}, z \rightarrow \infty) = 0$ can be represented as

$$\theta_j(\boldsymbol{\kappa}, z) = a_j(\boldsymbol{\kappa}, E) \exp[-q_1(\boldsymbol{\kappa}, E)z] + b_j(\boldsymbol{\kappa}, E) \exp[-q_2(\boldsymbol{\kappa}, E)z], \quad (6)$$

$$q_{1,2}(\boldsymbol{\kappa}, E) = \frac{1}{\sqrt{2}B} [A^2 - 2B\Xi(\boldsymbol{\kappa}) \pm \sqrt{A^4 - 4B\Xi A^2 + 4B^2 E^2}]^{1/2}. \quad (7)$$

The characteristic momenta $q_{1,2}(\boldsymbol{\kappa}, E)$ are the solutions of corresponding secular equation, $\kappa = |\boldsymbol{\kappa}|$. The boundary conditions (see Eq. (5)) determine the coefficients $a_j(\boldsymbol{\kappa}, E)$ and $b_j(\boldsymbol{\kappa}, E)$ as well as the dispersion relation $E(\boldsymbol{\kappa})$ for the near-surface states inside the bulk band gap, $|E(\boldsymbol{\kappa})| < \Xi$. The parameter $\lambda = A^2/4B\Xi$ is implied to be $\lambda \geq 1$.

Near-surface topological states. The potential $U(\boldsymbol{\kappa})$ in Eq. (5) is a 4×4 matrix specifying internal properties of the TI surface and the matrix elements $U_{jj'}(\boldsymbol{\kappa})$ include different components of scattering of the TI states on SP. Choosing the structure of the matrix and the strengths of its components allows us to tune spatial and energy characteristics of the topological states. In this Letter we consider the particular case when SP has only diagonal nonzero matrix elements: $U_{jj}(\boldsymbol{\kappa}) = U_j(\boldsymbol{\kappa})$ and $U_{jj'}(\boldsymbol{\kappa}) = 0$ for $j \neq j'$. In the following, for the sake of simplicity, we neglect the $U(\boldsymbol{\kappa})$ dependence on $\boldsymbol{\kappa}$. We focus on the SPs that preserve time reversal symmetry as well as the lattice translational symmetry in the plane of the surface. Therefore, in the following one can assume that $U_1 = U_3$ and $U_2 = U_4$ and, as a consequence, take in Eq. (6) $a_3 = \pm i e^{i\varphi} a_1$, $b_3 = \pm i e^{i\varphi} b_1$, $a_4 = \mp i e^{i\varphi} a_2$, $b_4 = \mp i e^{i\varphi} b_2$; $k_x \pm i k_y = \kappa e^{\pm i\varphi}$. We could interpret SP within the framework of a ‘‘local band bending’’ scheme where the band edge corresponding to the j -th spinor component is affected by the external perturbation confined at the surface: $\Xi \rightarrow \Xi \pm dU_j \delta(z)$. In the situation of TI coated with an external overlayer, the intuitive idea is that the diagonal components of SP could be heuristically adjusted to the relative offsets between corresponding energy levels (bands) of the TI substrate and the overlayer. In other words, the energy $dU_j \delta(z)$ mimics the local bend of corresponding bands.

After some algebra the secular equation results in the implicit cumbersome relation between the energy E and the in-plane momentum $\boldsymbol{\kappa}$. For arbitrary values of U_1 and U_2 and $\boldsymbol{\kappa} = 0$, the relation reduces to the equation:

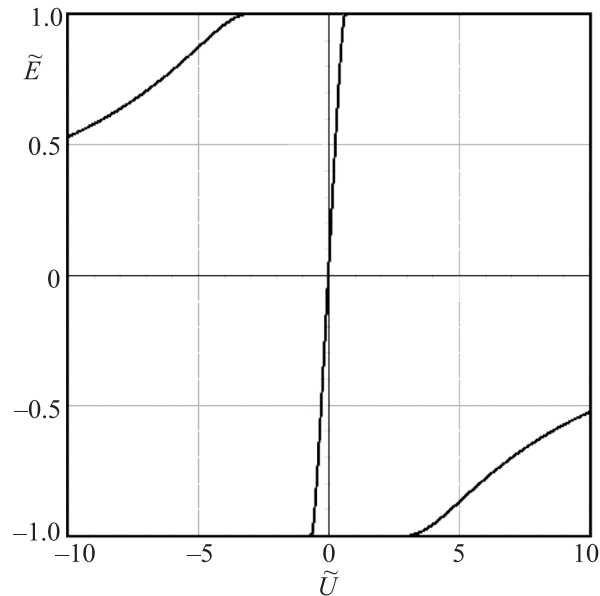
$$\frac{B}{2} \{ A^2 q_1(E) q_2(E) - [\Xi - E + B q_1^2(E)] [\Xi - E + B q_2^2(E)] \} +$$

$$+ [B q_1(E) q_2(E) - (\Xi - E)] \times \left\{ B^2 q_1(E) q_2(E) - dU_1 dU_2 - \frac{A^2}{4} \right\} -$$

$$- B [q_1(E) + q_2(E)] [dU_1 B q_1(E) q_2(E) + dU_2 (\Xi - E)] = 0, \quad (8)$$

where $q_{1,2}(E) = q_{1,2}(0, E)$. Note that Eq. (8) is invariant under the simultaneous permutations: $E \leftrightarrow -E$ and $U_1 \leftrightarrow -U_2$. The Eq. (8) determines the Dirac point position $E(\boldsymbol{\kappa} = 0)$ as a function of $U_{1,2}$: $E(\boldsymbol{\kappa} = 0) = E_0(U_{1,2})$.

The situation when $\text{sgn}(U_1 U_2) > 0$ could be ascribed to a sheet electrostatic field caused, for instance, by electron density redistribution at the surface or extrinsic gating. In the particular case of $U_1 = U_2 = U$, the dependence of the node point position on the SP strength, $E_0(U)$, obtained from Eq. (8), is plotted in Figure. If the potential gradually increases in magnitude,



The bound state node position within the gap, $\tilde{E} = E(\boldsymbol{\kappa} = 0)/\Xi$, versus the effective surface potential, $\tilde{U} = dU/\sqrt{B\Xi}$, at the band parameter $\lambda = 2$

one can see the following evolution. At weak potential $d|U| \ll \sqrt{B\Xi}$, the Dirac point linearly shifts with respect to the TI bulk bands to higher (for $U > 0$) or lower (for $U < 0$) binding energies. With the potential U approaching the values U_- or $-U_-$ the Dirac point moves upwards or downwards in energy and eventually merges into the conduction or valence bulk band continuum, respectively. Further, starting from the value U_+ or $-U_+$ the node point splits off the valence or conduction bulk band, respectively, and asymptotically approaches the

middle of the band gap. The threshold values of the potential are $\frac{2dU_{\pm}}{\sqrt{B\Xi}} = \sqrt{2(4\lambda-1)} \pm \sqrt{2(2\lambda-1)}$, so that $E_0(\pm U_{-}) = \pm\Xi$ and $E_0(\pm U_{+}) = \mp\Xi$.

To qualitatively interpret the situation with a pseudo-electric field, when $\text{sgn}(U_1 U_2) < 0$, let us imagine that, for example, an overlayer of trivial insulator In_2Se_3 is attached to Bi_2Se_3 substrate or the Bi content is partly substituted with In within the outermost QL in the truncated Bi_2Se_3 . It can lead to local reduction of the gap ($\Xi \rightarrow \Xi - d|U_{1,2}|\delta(z)$) and even to a non-inverted sequence of the energy terms near the TI surface due to artificial tuning of the strength of SOC. On the other hand, one can choose the overlayer material or substituting atoms which enhance SOC at the TI surface. One can show that in the case of the staggered alignment of the matrix elements, $U_1 = -U_2 = U$, when SP does not break the particle-hole symmetry, the near-surface state maintains the Dirac spectrum $E^{(\pm)}(\kappa) = \pm|A|\kappa$ regardless of the size and sign of U .

If the energy $\varepsilon(\kappa)$ is a small deviation from the Dirac linear spectrum, $E^{(\pm)}(\kappa) = \pm|A|\kappa + \varepsilon(\kappa)$, $|\varepsilon(\kappa)| \ll \Xi$, the characteristic momenta (see Eq. (7)) are given by

$$q_{1,2}^{(\pm)}(\kappa, E) = q_{1,2}^0(\kappa) + \frac{(\pm\kappa)\varepsilon(\kappa)}{Bq_{1,2}^0(\kappa)[q_{1,2}^0(\kappa) - q_{2,1}^0(\kappa)]}, \quad (9)$$

where $q_{1,2}^0(\kappa) = q_{1,2}(\kappa, |E| = |A|\kappa)$. The deviation $\varepsilon(\kappa)$ appears to be small when SP is either weak or strong. Using the expression (9) one can obtain the spectrum and estimate the spatial distribution of the near-surface state in these limit situations.

For the extremely large potential, $|U_{1,2}| \rightarrow \infty$, the correction approaches zero, $\varepsilon(\kappa) \rightarrow 0$, in turn, the EF coordinate dependence is described by a difference of the exponents, $\Theta(\boldsymbol{\kappa}, z) \sim \exp[-q_1^0(\kappa)z] - \exp[-q_2^0(\kappa)z]$, so that the maximum of the electron density, $\sim |\Theta(z)|^2$, does not occur on the surface, where $\Theta(z=0) = 0$, but rather near the point $z_0 \approx \ln(q_1^0/q_2^0)/(q_1^0 - q_2^0)$ (where $z_0 < \sqrt{B/\Xi} < (q_2^0)^{-1}$) that is distant from the surface. Such the EF distribution, together with the linear spectrum, was found under the free boundary conditions [30]. Our approach allows us to capture peculiarities of the surface state in 3D TI induced by the SP. If the SP size is much greater than the characteristic energy, $d|U_{1,2}| \gg Bq_1^0$, within the perturbation theory, one obtains the amendment to the linear dispersion law:

$$\varepsilon(\kappa) = -\frac{|A|}{\Xi(\kappa)} \left(\frac{1}{dU_1} + \frac{1}{dU_2} \right). \quad (10)$$

The surface state spectrum acquires a curvature and a shift of the node point, $E(\kappa = 0) = \varepsilon(0)$, which are inversely proportional to the potential, however the

fermion group velocity $|A|$ near the node point does not change since the amendment $\varepsilon(\kappa)$ (10) does not contain a linear in κ term. In the lowest order in $(U_{1,2})^{-1}$, the relations between the coefficients in (6) are given by

$$\begin{aligned} \frac{b_1(\kappa, E)}{a_1(\kappa, E)} &= -1 + \frac{\sqrt{A^2 - 4B\Xi(\kappa)}}{dU_1}, \\ \frac{b_2(\kappa, E)}{a_2(\kappa, E)} &= -1 - \frac{\sqrt{A^2 - 4B\Xi(\kappa)}}{dU_2}. \end{aligned} \quad (11)$$

Thus, the electron density does not vanish on the surface, $|\Theta(z=0)|^2 \sim (U_{1,2})^{-2}$. However, under the SP influence, the EF components can vanish near the surface at $z = z_{1,2} < z_0$, namely, $\theta_{1,3}(0, z) = 0$ at $z = z_1 = B/dU_1$ when $U_1 > 0$, and $\theta_{2,4}(0, z) = 0$ at $z = z_2 = -B/dU_2$ when $U_2 < 0$. Besides, as seen from Eq. (9), the SP affects the decay length of the EF nonzero harmonics.

If SP is formally absent, $U_1 = U_2 = 0$, one arrives at the solution obtained in Ref. [31] from using of the natural boundary conditions: the surface state shows the linear spectrum $E^{(\pm)}(\kappa) = \pm|A|\kappa$ and the EF spatial profile in z -direction is merely a sum of the exponents, $\Theta(\boldsymbol{\kappa}, z) \sim \exp[-q_1^0(\kappa)z] + \exp[-q_2^0(\kappa)z]$, i.e., the probability density of the near-surface state is peaked on the boundary $z = 0$ and its tail penetrates into the TI bulk with the decay length $\approx (q_2^0)^{-1}$. In the case of weak SP, $d|U_{1,2}| \ll \sqrt{B\Xi}$, the correction to the dispersion law is given by

$$\varepsilon(\kappa) = \frac{4|A|\Xi(\kappa)}{A^2 + 4B\Xi(\kappa)}(dU_1 + dU_2). \quad (12)$$

The spin-independent SP is seen to shift entirely and warp the energy-momentum dependence. Note, that the corrections (10) and (12) are opposite in the sign. Turning on the SP leads to the different contributions of the quick and slow exponents into EF: $b_j/a_j = 1 + o(U_{1,2})$.

In this Letter we avoid cumbersome analytical expressions and detailed plots concerning the spatial behavior of the near-surface states. Here we would emphasize only that the EF decay lengths, $\sim (q_1)^{-1}$ and $\sim (q_2)^{-1}$ (see Eq. (7)), are strongly influenced by the SP strength (except for the special case of $U_1 = -U_2$). For example, in the case of $U_1 = U_2 = U$, when the strength U varies either from 0 to $\pm U_{-}$ or from $\pm\infty$ to $\pm U_{+}$, the value $q_1(E)$ increases from $q_1^0(0)$ to $\sqrt{A^2 - 2B\Xi}/B$ and the value $q_2(E)$ decreases from $q_2^0(0)$ to 0.

Conclusion. Within the framework of the continual scheme we show how the envelope function spatial profile and the electron spectrum of the near-surface topological state vary depending on the type and strength of the surface potential. The appropriate effective sheet-like SP is associated with the surface perturbation; the

derived boundary conditions for EF, Eq. (5), involve directly the corresponding SP components. The method, conceptually presented here for the study of a semi-infinite semiconductor with inverted band gap covered with an atomically thin non-magnetic insulating overlayer, can be straightforwardly extended to solve a wide range of problems related to a behavior of 3D TIs under the surface perturbations. This approach is attractive due to a relative calculating simplicity and a transparent physical interpretation. Thus our work opens up new horizons towards studying and engineering topological electronic phases in the 3D TI based structures.

We acknowledge support by the Ministry of Education and Science of Russian Federation (state task #2.8575.2013), the Federal Targeted Program “Scientific and scientific-pedagogical personnel of innovative Russia in 2009-2013” (#14.B37.21.1164), and the Russian Foundation for Basic Researches (grant #13-02-00016).

1. M. Z. Hasan and C. L. Kane, *Rev. Mod. Phys.* **82**, 3045 (2010).
2. J. E. Moore, *Nat. Phys.* **5**, 378 (2009).
3. T. Okuda and A. Kimura, *J. Phys. Soc. Jpn.* **82**, 021002 (2013).
4. I. Garate and M. Franz, *Phys. Rev. Lett.* **104**, 146802 (2010).
5. R. Yu, W. Zhang, H.-J. Zhang, S.-C. Zhang, X. Dai, and Z. Fang, *Science* **329**, 61 (2010).
6. T. Fujita, M. B. A. Jalil, and S. G. Tan, *Applied Physics Express* **4**, 094201 (2011).
7. L. A. Wray, S. Xu, Y. Xia, D. Hsieh, A. V. Fedorov, Y. S. Hor, R. J. Cava, A. Bansil, H. Lin, and M. Z. Hasan, *Nat. Phys.* **7**, 32 (2011).
8. M. R. Scholz, J. Sanchez-Barriga, D. Marchenko, A. Varykhalov, A. Volykhov, L. V. Yashina, and O. Rader, *Phys. Rev. Lett.* **108**, 256810 (2012).
9. T. Valla, Z.-H. Pan, D. Gardner, Y. S. Lee, and S. Chu, *Phys. Rev. Lett.* **108**, 117601 (2012).
10. D. Kong, J. J. Cha, K. Lai, H. Peng, J. G. Analytis, S. Meister, Y. Chen, H.-J. Zhang, I. R. Fisher, Z.-X. Shen, and Y. Cui, *ACS Nano* **5**, 4698 (2011).
11. S. V. Eremeev, G. Landolt, T. V. Menshchikova, B. Slomski, Y. M. Koroteev, Z. S. Aliev, M. B. Babanly, J. Henk, A. Ernst, L. Patthey, A. Eich, A. A. Kha-jetoorians, J. Hagemeister, O. Pietzsch, J. Wiebe, R. Wiesendanger, P. M. Echenique, S. S. Tsirkin, I. R. Amiraslanov, J. H. Dil, and E. V. Chulkov, *Nat. Commun.* **3**, 635 (2012).
12. L. Miao, Z. F. Wang, W. Ming, M.-Y. Yao, M. Wang, F. Yang, Y. R. Song, F. Zhu, A. V. Fedorov, Z. Sun, C. L. Gao, C. Liu, Q.-K. Xue, C.-X. Liu, F. Liu, D. Qian, and J.-F. Jia, *Proceedings of the National Academy of Sciences* **110**, 2758 (2013).
13. G. S. Jenkins, A. B. Sushkov, D. C. Schmadel, A. B. Sushkov, H. D. Drew, M. Bichler, G. Koblmüller, M. Brahlek, N. Bansal, and S. Oh, arXiv:1208.3881.
14. M. H. Berntsen, O. Götberg, and O. Tjernberg, *Phys. Rev. B* **87**, 155126 (2013).
15. J. Chen, H. J. Qin, F. Yang, J. Liu, T. Guan, F. M. Qu, G. H. Zhang, J. R. Shi, X. C. Xie, C. L. Yang, K. H. Wu, Y. Q. Li, and L. Lu, *Phys. Rev. Lett.* **105**, 176602 (2010).
16. J. G. Checkelsky, Y. S. Hor, R. J. Cava, and N. P. Ong, *Phys. Rev. Lett.* **106**, 196801 (2011).
17. M. Bianchi, R. C. Hatch, J. Mi, B. B. Iversen, and P. Hofmann, *Phys. Rev. Lett.* **107**, 086802 (2011).
18. M. S. Bahramy, P. D. C. King, A. de la Torre, J. Chang, M. Shi, L. Patthey, G. Balakrishnan, Ph. Hofmann, R. Arita, N. Nagaosa, and F. Baumberger, *Nat. Commun.* **3**, 1159 (2012).
19. C. Pauly, G. Bihlmayer, M. Liebmann, M. Grob, A. Georgi, D. Subramaniam, M. R. Scholz, J. Sánchez-Barriga, A. Varykhalov, S. Blügel, O. Rader, and M. Morgenstern, *Phys. Rev. B* **86**, 235106 (2012).
20. S. V. Eremeev, M. G. Vergniory, T. V. Menshchikova, A. A. Shaposhnikov, and E. V. Chulkov, *New J. Phys.* **14**, 113030 (2012).
21. S. V. Eremeev, G. Bihlmayer, M. Vergniory, Yu. M. Koroteev, T. V. Menshchikova, J. Henk, A. Ernst, and E. V. Chulkov, *Phys. Rev. B* **83**, 205129 (2011).
22. Q. Zhang, Z. Zhang, Z. Zhu, U. Schwingenschlogl, and Y. Cui, *ASC NANO* **6**, 2345 (2012).
23. G. Wu, H. Chen, Y. Sun, X. Li, P. Cui, C. Franchini, J. Wang, X.-Q. Chen, and Z. Zhang, *Scientific Reports* **3**, 1233 (2013).
24. L. Zhao, J. Liu, P. Tang, and W. Duan, *Appl. Phys. Lett.* **100**, 131602 (2012).
25. C. Chena, S. Hea, H. Weng, W. Zhang, L. Zhao, H. Liu, X. Jia, D. Mou, S. Liu, J. He, Y. Peng, Y. Feng, Z. Xie, G. Liu, X. Dong, J. Zhang, X. Wang, Q. Peng, Z. Wang, S. Zhang, F. Yang, C. Chen, Z. Xu, X. Dai, Z. Fang, and X. J. Zhou, *PNAS* **109**, 3694 (2012).
26. S. V. Eremeev, Yu. M. Koroteev, and E. V. Chulkov, *JETP Lett.* **91**, 387 (2010).
27. G. L. Bir and G. E. Pikus, *Symmetry and Strain-Induced Effects in Semiconductors*, J. Wiley & Sons, New York, Keter Publishing House, Jerusalem (1974) [Simmetriya i deformatsionnye efekty v poluprovodnikakh, M., Nauka, 1972].
28. H. Zhang, C. Liu, X. Qi, X. Dai, Z. Fang, and S. Zhang, *Nat. Phys.* **5**, 438 (2009).
29. C. X. Liu, X. L. Qi, H. J. Zhang, X. Dai, Z. Fang, and S.-C. Zhang, *Phys. Rev. B* **82**, 045122 (2010).
30. W.-Y. Shan, H.-Z. Lu, and S.-Q. Shen, *New J. Phys.* **12**, 043048 (2010).
31. A. Medhi and V. B. Shenoy, *J. Phys. Cond. Mat.* **24**, 355001 (2012).
32. V. A. Volkov and T. N. Pinskiy, *Sov. Phys. Solid State* **23**, 1022 (1981).